CDF Note 7115

Time-Dependent Angular Analysis of $B_s \to J/\psi\phi$ and $B_d \to J/\psi K^{*0}$ Decays and a Lifetime Difference in the B_s System

The CDF Collaboration
URL http://www-cdf.fnal.gov/physics/new/bottom/040708.blessed-dgog-bsjpsiphi/

(Dated: March 4, 2005)

We present results from a combined analysis of lifetimes and transversity amplitudes for $B_s \to J/\psi\phi$ and $B_d \to J/\psi K^{*0}$ decays using CDF Run II data up to February 13, 2004. For B_s, we obtain:

$$
\begin{aligned}
A_0 &= 0.784 \pm 0.039 \pm 0.007 \\
A_{||} &= (0.510 \pm 0.082 \pm 0.013) e^{(1.94 \pm 0.36 \pm 0.03)i} \\
|A_\perp| &= 0.354 \pm 0.098 \pm 0.003 \\
\tau_L &= 1.05\,^{+0.16}_{-0.13} \pm 0.02 \text{ ps} \\
\tau_H &= 2.07\,^{+0.58}_{-0.46} \pm 0.03 \text{ ps} \\
\Delta\Gamma/\Gamma &= 0.65\,^{+0.25}_{-0.33} \pm 0.01 \\
\Delta\Gamma &= 0.47\,^{+0.19}_{-0.24} \pm 0.01 \text{ ps}^{-1}
\end{aligned}
$$

For B_d, we obtain:

$$
\begin{aligned}
A_0 &= 0.750 \pm 0.017 \pm 0.012 \\
A_{||} &= (0.473 \pm 0.034 \pm 0.006) e^{(2.86 \pm 0.22 \pm 0.07)i} \\
A_\perp &= (0.464 \pm 0.035 \pm 0.007) e^{(0.15 \pm 0.15 \pm 0.04)i} \\
\tau_{B_d} &= 1.54 \pm 0.05 \pm 0.02 \text{ ps}
\end{aligned}
$$

Final results, accepted for publication in PRL

I. INTRODUCTION

The mixing phenomenon in the system of neutral B mesons (B_d, B_s) gives rise to two eigenstates of definite masses (heavy, m_H and light, m_L) and widths (Γ_H and Γ_L) such that the time evolution of these eigenstates is given by $\exp(-im_{L,H}t - \frac{\Gamma_{L,H}}{2}t)$. It is convenient to define $\Delta m \equiv m_H - m_L \geqslant 0$, $\Gamma \equiv \frac{1}{2}(\Gamma_L + \Gamma_H)$ and $\Delta\Gamma \equiv \Gamma_L - \Gamma_H \geqslant 0$. Theoretical expectations are that the decay width difference is very small in the B_d system but that it could be sizeable in the B_s system [1].

In this analysis we study the $B_d \to J/\psi K^{*0}$ and $B_s \to J/\psi\phi$ decay modes, with $J/\psi \to \mu^+\mu^-$, $K^{*0} \to K^+\pi^-$, and $\phi \to K^+K^-$. Through a time-dependent analysis of the decay amplitudes we are able to look for a lifetime difference, $\frac{\Delta\Gamma}{\Gamma}$, in the B_s system by exploiting the fact that the decay occurs through both CP even and odd amplitudes and that these amplitudes are associated with the Light and Heavy CP eigenstates. A similar analysis for the B_d system provides important cross checks for the results obtained in the B_s system.

II. DATA SAMPLE & EVENT SELECTION

Events used in this analysis were collected with the upgraded Collider Detector (CDF II) at the Tevatron $p\overline{p}$ collider, from February 2002 to February 2004, and come from a data set with an integrated luminosity of $\sim 260\,\mathrm{pb}^{-1}$. As described in detail in Ref. [6], CDF consists of a precision magnetic spectrometer surrounded by calorimeters and muon chambers. The components relevant to this analysis are briefly described here. CDF uses a cylindrical coordinate system in which the postive z axis starts at the center of the detector and points in the direction of the proton beam, r is the radial distance transverse to the beam, and ϕ is the azimuthal angle about the beam line. A cylindrical drift chamber (COT) provides 96 measurements, between radii of 40 and 137 cm, organized into alternating axial and stereo ($\pm 2°$) super-layers [7]. A 5 layer double-sided silicon microstrip detector (SVXII) provides precise ($\sim 15\mu$m) measurements, at radii between 2.5 and 10.6 cm [8]. Both detectors are immersed in a nearly uniform axial 1.4 T magnetic field, allowing precision measurement of p_T, the momenta of charged particles in the plane transverse to the beamline. Planar drift chambers identify muons with $p_T > 1.4$ GeV/c which penetrate the calorimeter within 40° of the the transverse direction [10].

The data used in this analysis were selected by a dimuon trigger. Muons were required to have $p_T > 1.5$ GeV/c and be separated in ϕ by 2.5°. About 2 million oppositely charged muon pairs are obtained having a mass within 80 MeV/c^2 of the PDG value for the J/ψ mass. B meson candidates are reconstructed by including kaon and pion candidate tracks with $p_T > 400$ MeV/c. Each of the four charged particles (muons, kaons and pions) are required to have at least 3 axial measurements in SVXII and at least 5 measurements in each of at least 2 axial and 2 stereo super-layers in the COT. The dimuons are constrained to the PDG value for the J/ψ mass in the 3D four-track vertex fit.

For the B_d candidates, the $K\pi$ mass is required to be within 50 MeV/c^2 of the PDG K^{*0} mass, with the K^{*0} $p_T > 2.6$ GeV/c and the B_d $p_T > 6.0$ GeV/c. When multiple $K - \pi$ assignments are possible, the assignment giving the $K\pi$ mass closest to the PDG K^{*0} mass is chosen. For the B_s candidates, the K^+K^- mass is required to be within 6.5 GeV/c^2 of the PDG ϕ mass, with the ϕ $p_T > 2.0$ GeV/c and the B_s $p_T > 6.5$ GeV/c.

The lifetime can be determined from the distribution of the proper decay length (PDL). In this analysis the proper decay length is determine by the transverse distance of the four track secondary vertex from the beamline, signed relative to the direction of the transverse momentum of the B candidate. The position and orientation of the beamline is determined from inclusive jet trigger data. The transverse size of the beam spot is $\sim 30\mu$m.

III. TIME-DEPENDENT ANGULAR ANALYSIS

A. Transversity Amplitudes

Reference [2] gives the differential decay rate at time t for the $J/\psi(\mu^+\mu^-)K^{*0}(K^+\pi^-)$ and $J/\psi((\mu^+\mu^-)\phi(K^+K^-)$ modes:

$$\begin{aligned}\frac{d^4\mathcal{P}(\vec{\rho},t)}{d\vec{\rho}\,dt} &\propto |A_0|^2 \cdot g_1(t) \cdot f_1(\vec{\rho}) + |A_\parallel|^2 \cdot g_2(t) \cdot f_2(\vec{\rho}) \\ &+ |A_\perp|^2 \cdot g_3(t) \cdot f_3(\vec{\rho}) \pm Im(A_\parallel^* A_\perp) \cdot g_4(t) \cdot f_4(\vec{\rho}) \\ &+ Re(A_0^* A_\parallel) \cdot g_5(t) \cdot f_5(\vec{\rho}) \pm Im(A_0^* A_\perp) \cdot g_6(t) \cdot f_6(\vec{\rho})\end{aligned} \quad (1)$$

in which $\vec{\rho} = (\cos\theta, \varphi, \cos\psi)$ and the angles θ, φ, and ψ are defined in the transversity basis, and $f_{1,\ldots,6}(\vec{\rho})$ are defined as follows:

$$\begin{aligned}
f_1(\vec{\rho}) &= \frac{9}{32\pi} 2\cos^2\psi(1-\sin^2\theta\cos^2\varphi) \\
f_2(\vec{\rho}) &= \frac{9}{32\pi}\sin^2\psi(1-\sin^2\theta\sin^2\varphi) \\
f_3(\vec{\rho}) &= \frac{9}{32\pi}\sin^2\psi\sin^2\theta \\
f_4(\vec{\rho}) &= -\frac{9}{32\pi}\sin^2\psi\sin 2\theta\sin\varphi \\
f_5(\vec{\rho}) &= \frac{9}{32\pi}\frac{1}{\sqrt{2}}\sin 2\psi\sin^2\theta\sin 2\varphi \\
f_6(\vec{\rho}) &= \frac{9}{32\pi}\frac{1}{\sqrt{2}}\sin 2\psi\sin 2\theta\cos\varphi
\end{aligned} \tag{2}$$

The transversity basis is defined in the rest frame of the J/ψ. The K^{*0} flight direction defines positive x axis, while the plane of $K\pi$ system defines the $x-y$ plane with y axis such that $p_y(K) > 0$. The z axis is chosen to form a right-handed coordinate system. The transversity angle, θ, is the angle between the μ^+ flight direction and the z axis. The angle φ is the angle between the x-axis and the projection of the μ^+ flight direction onto the $x-y$ plane. The angle ψ is the (helicity) angle of the K in the K^{*0} rest frame relative to the negative of the direction of the J/ψ in that frame. These definitions carry over directly for the case of $B_s \to J/\psi\phi$ decay (where the ϕ flight direction defines the x axis and and $p_y(K^+) > 0$).

The three decay amplitudes correspond to linear polarizations [3] of the vector mesons which are either longitudinal (A_0), or transverse to their flight direction and parallel or perpendicular to one another ($A_\parallel$ and $A_\perp$, respectively). The amplitude $A_\perp$ is associated with decays in which the two vector mesons are emitted with relative orbital angular momentum $l = 1$ and therefore with parity (CP) odd decays in the B_d (B_s) channel. The amplitudes A_0 and $A_\parallel$ are associated with (mixtures of) the $l = 0$ and 2 decays which are parity (CP) even.

Equation 1 is valid for initially produced B ($\overline{B}$) mesons when the upper (lower) sign is taken for the interference terms (4 and 6) between the parity (CP) even and odd amplitudes. The time evolution of the angular decay terms, the $g_i(t)$'s, depends on whether a B or a $\overline{B}$ is initially produced and the evolution of the state through mixing and decays after production.

In the B_s system, the mass eigenstates are nearly CP eigenstates and so are the observed final states. The CP-even angular decay terms (involving $A_{0,\parallel}$) evolve in time with $e^{-\Gamma_L t}$, while the CP-odd angular decay terms (depending on $A_\perp$) evolve with $e^{-\Gamma_H t}$. The observed time-dependent angular distribution is obtained by summing the distributions for initially produced B_s and $\overline{B}_s$ mesons. The resulting cancellation of the terms involving interference between the CP even and odd decays leaves:

$$\begin{aligned}
\frac{d^4\mathcal{P}(\vec{\rho},t)}{d\vec{\rho}\,dt} \propto & |A_0|^2 e^{-\Gamma_L t}\cdot f_1(\vec{\rho}) + |A_\parallel|^2 e^{-\Gamma_L t}\cdot f_2(\vec{\rho}) \\
& + |A_\perp|^2 e^{-\Gamma_H t}\cdot f_3(\vec{\rho}) + \mathrm{Re}(A_0^* A_\parallel) e^{-\Gamma_L t}\cdot f_5(\vec{\rho})
\end{aligned} \tag{3}$$

With Equation 3 it is possible to extract $|A_{0,\parallel,\perp}|$, Γ_L, Γ_H and $\delta_\parallel$. However, unlike for B_d (discussed below), information on $\delta_\perp$ can not be extracted.

In the B_d system the mass eigenstates are not CP eigenstates; $\delta\phi_d = 2\beta$ and $\sin(2\beta) \approx 3/4$. Therfore, when omitting the oscillation terms the CP-even amplitudes evolve as $\cos^2\beta e^{-\Gamma_L t} + \sin^2\beta e^{-\Gamma_H t}$ and the CP-odd amplitude as $\sin^2\beta e^{-\Gamma_L t} + \cos^2\beta e^{-\Gamma_H t}$ [4]. In principle this still leaves a sensitivity to the first order in $\Delta\Gamma_d$ but by observing flavor-specific B_d decays the sensitivity to $\Delta\Gamma_d$ is reduced to second order [5].

Summing over initially produced B_d and $\overline{B}_d$ decays gives:

$$\begin{aligned}
\frac{d^4\mathcal{P}(\vec{\rho},t)}{d\vec{\rho}\,dt} \propto & \Big[|A_0|^2\cdot f_1(\vec{\rho}) + |A_\parallel|^2\cdot f_2(\vec{\rho}) \\
& + |A_\perp|^2\cdot f_3(\vec{\rho}) \pm \mathrm{Im}(A_\parallel^* A_\perp)\cdot f_4(\vec{\rho}) \\
& + \mathrm{Re}(A_0^* A_\parallel)\cdot f_5(\vec{\rho}) \pm \mathrm{Im}(A_0^* A_\perp)\cdot f_6(\vec{\rho})\Big] e^{-\Gamma_d t}
\end{aligned} \tag{4}$$

where the upper(lower) is used for the flavor specific final state of the K^{*0}, $K^+\pi^-$ ($K^-\pi^+$).

B. Unibinned Likelihood Technique

An unbinned Likelihood fit is performed in terms of the mass, proper decay length and transversity angular variables. The Likelihood function includes terms for signal and background, and in the B_d decays, terms for 'swapped' events in which the a candidate has survived desite an interchange in the correct $K\pi$ particle ID assignment. This latter class of events consititutes about 10% of the B_d signal and is a tractable nuisance. The probability density function includes convolution with a Gaussian resolution function based on the event by event uncertainty in the reconstructed proper decay length. The mass resolution is also handled on an event by event basis. Scale factors for the proper decay length and mass uncertainties are included. Where appropriate the Likelihood fit allows for the possibility of additional (positive and negative) exponential tails in the proper decay length distribution describing the background.

The angular distribution of both the signal and the background are modeled using the transversity angular terms described above, with the background described by a separate set of 'amplitudes'. The observed angular distribution is sculpted by the acceptance and efficiency of the detector, trigger and selection criteria. The dominant contribution to the sculpting is the kinematic selection criteria (p_T cuts) imposed by the trigger. A technique for correcting for the this sculpting without a priori knowledge of the decay amplitudes is employed through the use of partial normalization factors in the Likelihood function that have been determined by reconstructing Monte Carlo events tossed according to phase space and thus flat in the appropriate tranversity variables [12].

IV. RESULTS

Mass and proper decay length projection plots for the B_d and B_s fit are shown in Figures 1 and 2. Figure 3 shows the sideband subtracted projections for the $K^{*0} \to K\pi$ and $\phi \to K^+K^-$ distributions. Figure 4 and Figure 5 show the $K\pi$ and K^+K^- distributions for the B signal (within $\pm 2.5\sigma$) and sideband regions (beyond $\pm 5\sigma$) after the four track vertex fit. Note that the enhancement in the $K\pi$ sideband distribution near the K^{*0} mass is an understood result of the $K\pi$ mass assignment and selection of the track pair having the closest mass to the PDG value for the K^{*0} mass.

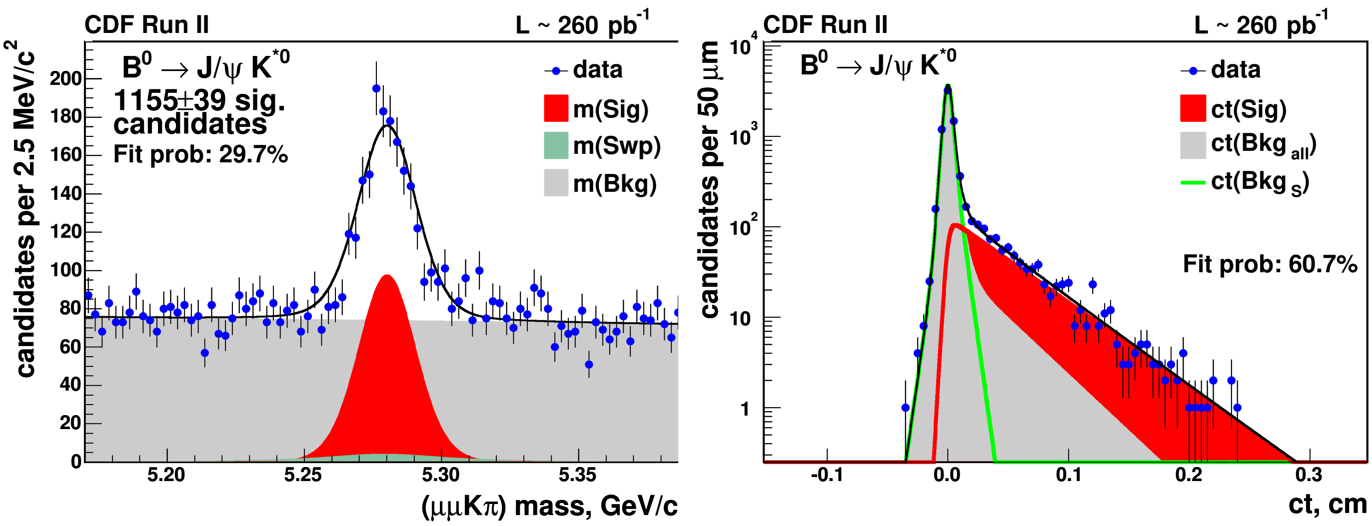

FIG. 1: Projection of the results of the unbinned Likelihood fit onto the data for $B0 \to J/\psi K^{*0}$. Probability of the χ^2 compatibility test is indicated on each plot.

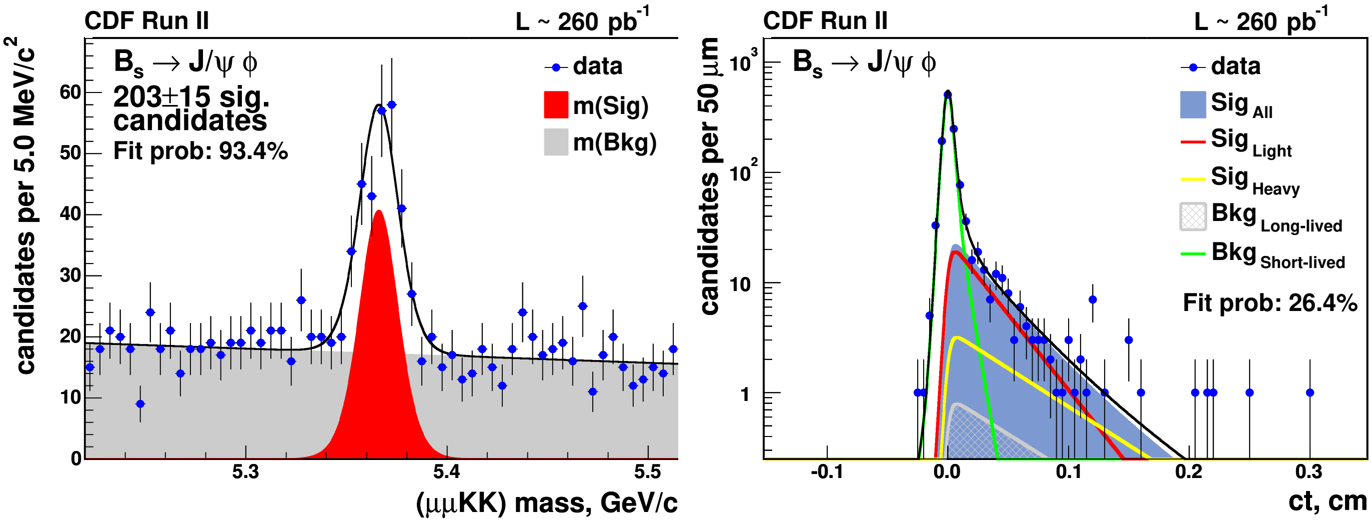

FIG. 2: Projection of the results of the unbinned Likelihood fit onto the data for $B_s \to J/\psi\phi$. Probability of the χ^2 compatibility test is indicated on each plot.

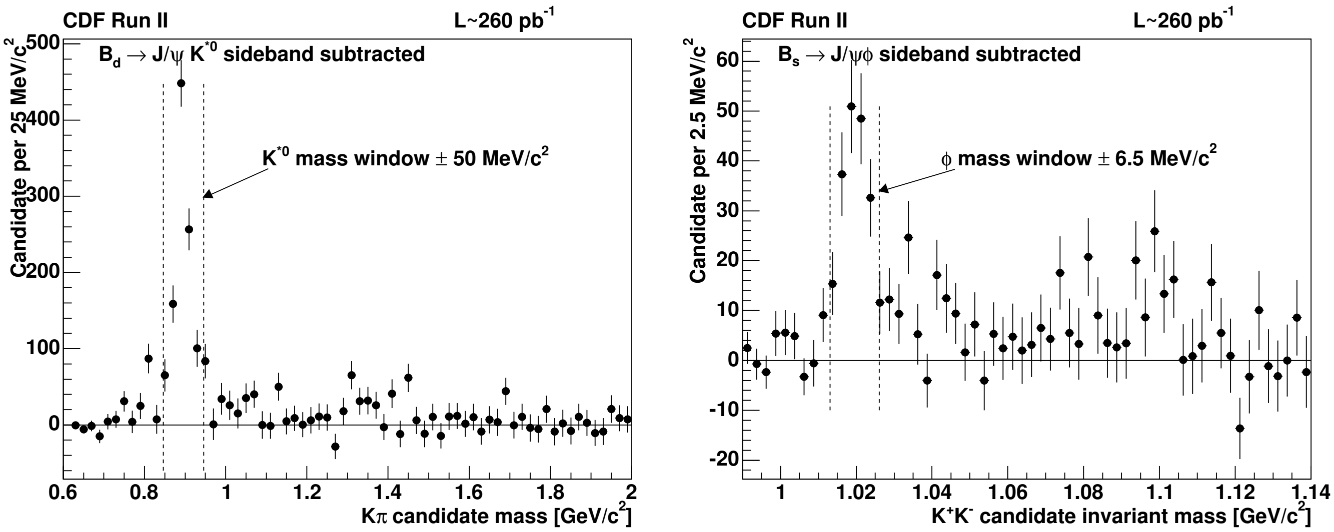

FIG. 3: Sideband subtracted mass spectra showing $K^* \to K\pi$ for the B_d data (left) $\phi \to K^+K^-$ for the B_s data (right).

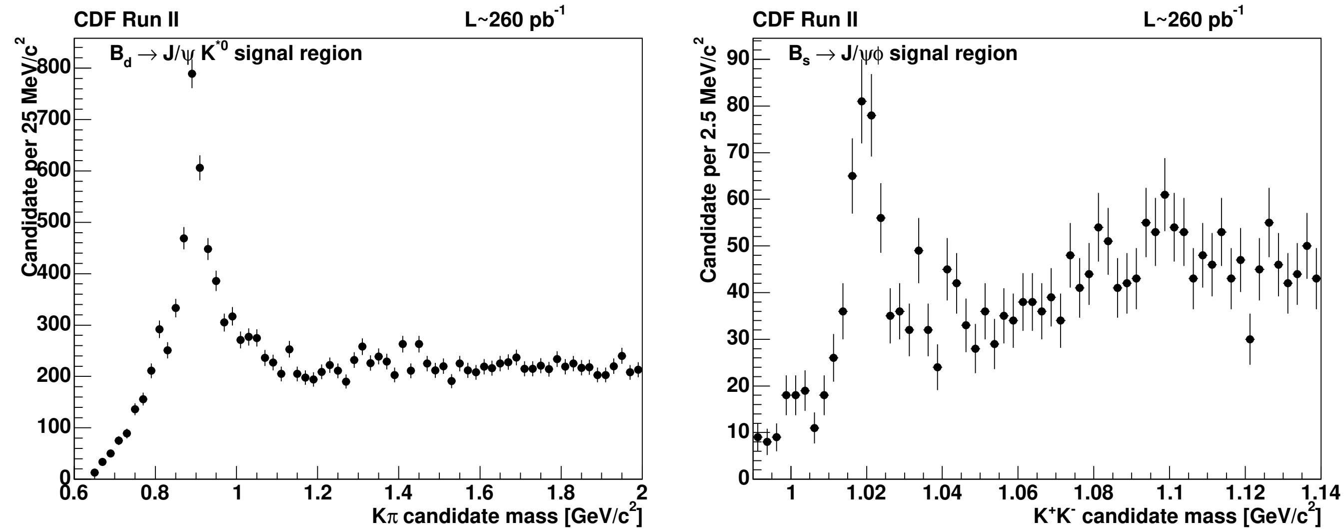

FIG. 4: $K\pi$ mass distribution for the B_d (left) and K^+K^- mass distribution for the B_s data (right) in the B signal region ($\pm 2.5\sigma$).

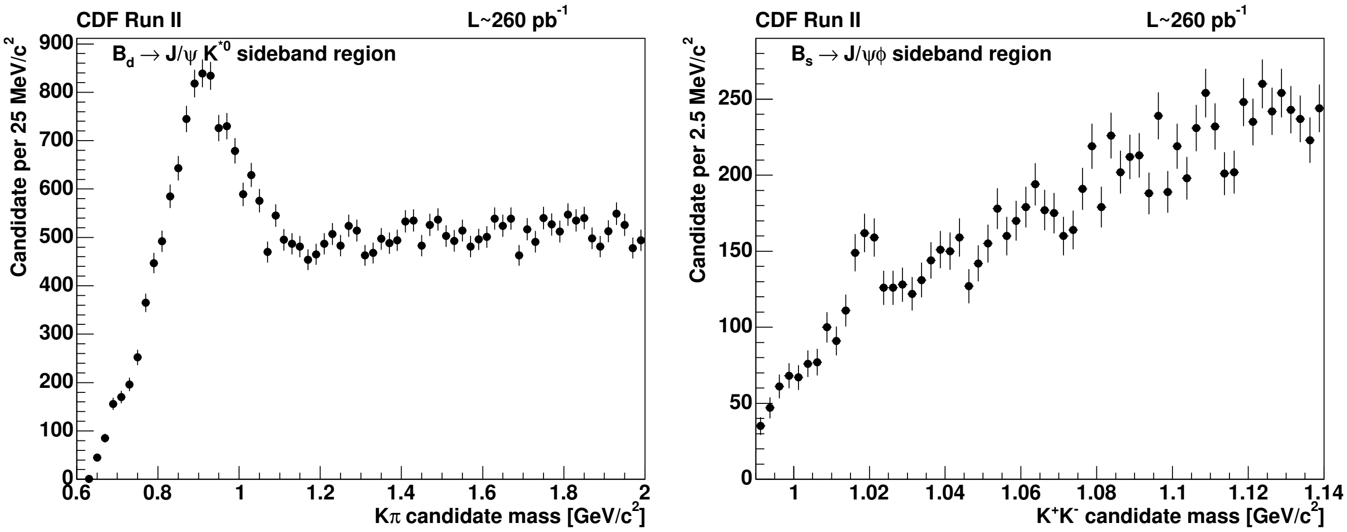

FIG. 5: $K\pi$ mass distribution for the B_d data (left) and K^+K^- mass distribtuion for the B_s data (right) in the B sideband region (beyond 5 σ).

Figures 6 and 7 show projections for the fits and data of the transversity angular distributions. These projections are made using sideband subtracted data (for $c\tau > 0$) and corrected for detector acceptance.

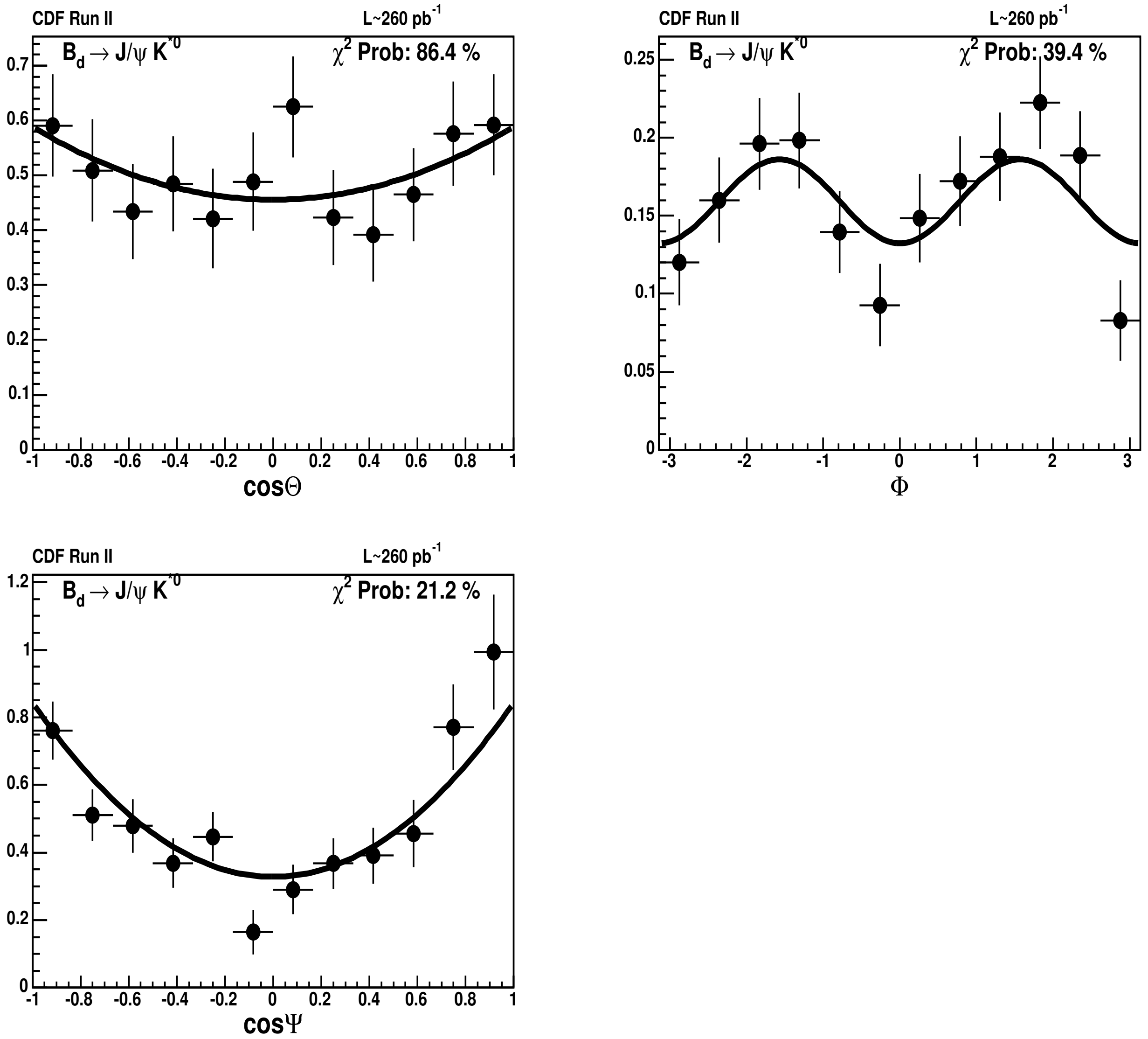

FIG. 6: The projection plots of the fit results to the sideband subtracted angular distributions, corrected for acceptance of B_d candidates for $c\tau > 0$. The data (points) and fit projection curves are each normalized to unity.

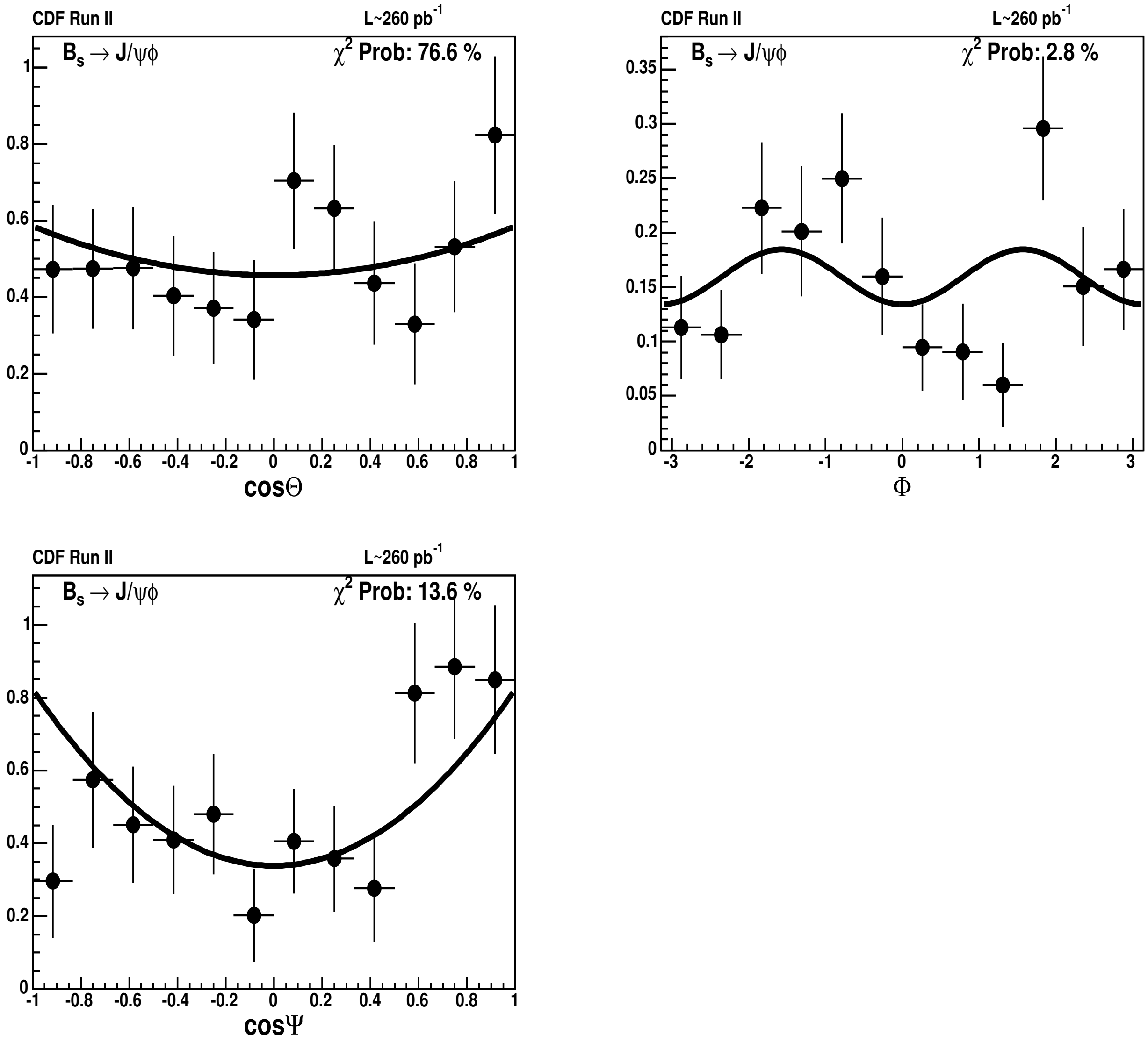

FIG. 7: The projection plots of the fitting results to the sideband subtracted angular distributions, corrected for acceptance of B_s candidates for $c\tau > 0$. The data (points) and fit projection curves are each normalized to unity.

A. Results of the Likelihood Fits

Numerical results from the time-dependent angular fits are given in Tables I and II. Because the B_s decay is not self-tagging the phase $\delta_\perp$ is not accessible. In the B_s fits, two of the quantities of interest, *e.g.* $c\tau_L$ and $c\tau_H$ or $c\tau_L$ and $\frac{\Delta\Gamma}{\Gamma}$, are free parameters; multiple fits are performed to obtain direct results for each quantity. The B_s constrained fit requires equality of the total decay rates for B_s and B_d, that is $\Gamma_s = \Gamma_d = 1/c\tau_d$, to within 1%.

For reference, the full unbinned Likelihood result for the time-dependent angular fit for B_s allowing only one lifetime returns a value of $c\tau_{B_s \to J/\psi\phi} = 395\ ^{+33}_{-30}\mu$m. This value is NOT to be confused with $c\tau_s = 1/\Gamma_s$, because branching fractions to CP even and odd eigenstate are not representative of all B_s decays.

	B_d	B_s Unconstrained Fit	B_s Constrained Fit	unit
M_B	5280.2 ± 0.8	5366.1 ± 0.8	5366.0 ± 0.8	MeV/c^2
A_0	0.750 ± 0.017	0.784 ± 0.039	0.783 ± 0.038	
$A_\parallel$	0.473 ± 0.034	0.510 ± 0.082	0.539 ± 0.070	
$A_\perp$	0.464 ± 0.035	0.354 ± 0.098	0.308 ± 0.087	
$\delta_\parallel$	2.86 ± 0.22	1.94 ± 0.36	1.91 ± 0.32	
$\delta_\perp$	0.15 ± 0.15			
$c\tau_B$	462 ± 15			μm
$c\tau_L$		$316\ ^{+48}_{-40}$	$340\ ^{+40}_{-28}$	μm
$c\tau_H$		$622\ ^{+175}_{-138}$	$713\ ^{+167}_{-129}$	μm
$c\tau_s$		$419\ ^{+45}_{-38}$	$\mathbf{460 \pm 6.2}$	μm
$\Delta\Gamma_s/\Gamma_s$		$65\ ^{+25}_{-33}$	$71\ ^{+24}_{-28}$	%
$\Delta\Gamma_s$		$0.47\ ^{+0.19}_{-0.24}$	$0.46\ ^{+0.17}_{-0.18}$	ps^{-1}
N_{sig}	1155 ± 39	203 ± 15	201 ± 15	

TABLE I: Main Fit Results: the reconstructed mass, the three decay amplitudes $A_0, A_\parallel, A_\perp$ and the relative phase of the second two with the first (which can be taken as real), the measured lifetime (PDL), $\frac{\Delta\Gamma}{\Gamma}$ and $\Delta\Gamma$ (for the B_s decays), and the number of signal events.

Parameter	B_d result	B_s result	unit
f_s	0.151 ± 0.005	0.164 ± 0.012	
A	-1.06 ± 0.89	-2.2 ± 1.2	(GeV/c^2)$^{-1}$
S_m	1.65 ± 0.06	1.81 ± 0.12	
$\lvert B_0\rvert^2$	0.292 ± 0.009	0.318 ± 0.023	
$\lvert B_\parallel\rvert^2$	0.358 ± 0.017	0.385 ± 0.041	
$arg(B_\parallel)$	1.60 ± 0.06	1.63 ± 0.13	
f_-	0.042 ± 0.014	———	
f_+	0.145 ± 0.019	0.124 ± 0.031	
f_{++}	0.044 ± 0.006	0.011 ± 0.007	
λ_-	47 ± 7	———	μm
λ_+	45 ± 6	66 ± 17	μm
λ_{++}	348 ± 40	634 ± 280	μm
S_{ct}	1.27 ± 0.02	1.33 ± 0.04	

TABLE II: Other Fit Parameters: the signal fraction, background shape parameters and scale factors for the mass and proper decay length resolution.

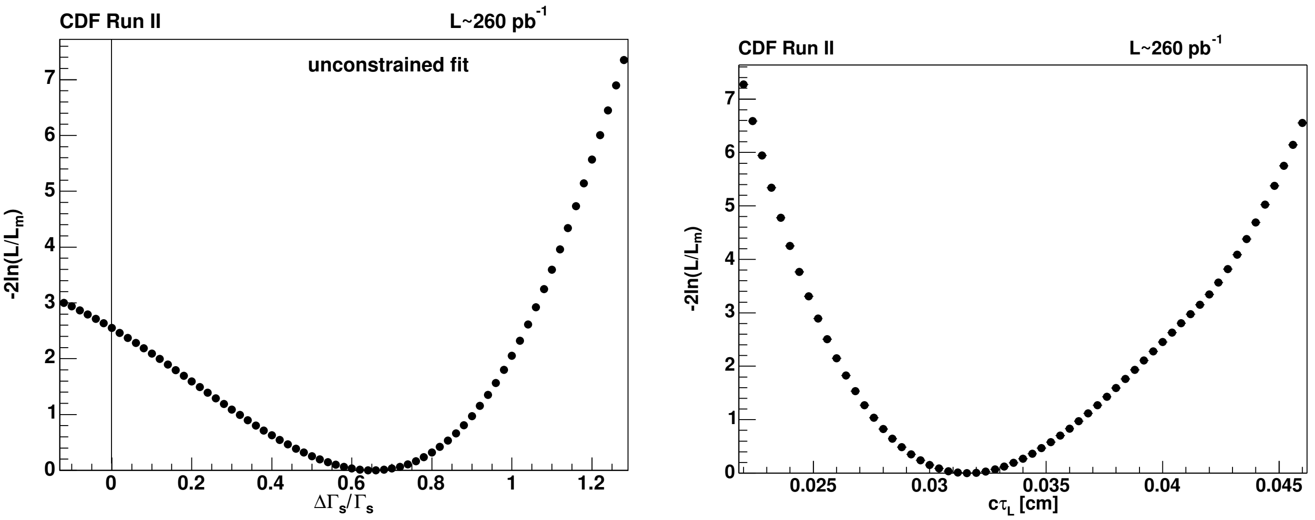

FIG. 8: Scan of the Likelihood function for $\Delta\Gamma_s/\Gamma_s$ for the unconstrained fit (left), and scan of the Likelihood function for $c\tau_L$ for the unconstrained fit (right).

V. DISCUSSION OF CONSTRAINED FITS

Fits are made using the constraint, $\tau_s = 2\tau_H\tau_L/(\tau_H + \tau_L) = \tau_d$. The constraint value used is based on the PDG 2004 result for $c\tau_d = 460.8 \pm 4.2$ μm with an additional 1% systematic uncertainy added in quadrature to relfect the theoretical (un)certainty that the B_d and B_s total decay widths should be equal to within 1%.

Figures 8 shows a scan of the Likelihood function for $\Delta\Gamma_s/\Gamma_s$ and $c\tau_L$ for the unconstrained fit. Figure 9 shows a scan of the Likelihood function for $\Delta\Gamma_s/\Gamma_s$ and the proper decay length projection for the constrained fit.

The values obtained directly from the Likelihood scan are given in Table III.

Likelihood Scan Value	$\Delta\Gamma_s/\Gamma_s = 0$	$\Delta\Gamma_s/\Gamma_s = 0.12$
Unconstrained Fit	2.55	1.99
Constrained Fit	5.69	3.95

TABLE III: Likelihood Scan Value.

An interesting question to ask is how likely it would be for an ensemble of experiments with similar statistical sensitivity to observe a value for $\frac{\Delta\Gamma}{\Gamma}$ as large as we observed if Nature provides us with no lifetime difference ($\frac{\Delta\Gamma}{\Gamma} = 0$) or the Standard Model prediction [5] for $\frac{\Delta\Gamma}{\Gamma} = 12 \pm 6\%$. From Monte Carlo studies:

- For pseudo-experiments tossed with $\frac{\Delta\Gamma}{\Gamma} = 0$
  - For the unconstrained fit:
    betting odds: $< 1/315$
  - For the constrained fit:
    betting odds: $< 1/718$
- For pseudo-experiments tossed with $\frac{\Delta\Gamma}{\Gamma} = 0.12$
  - For the unconstrained fit:
    betting odds: $< 1/84$
  - For the constrained fit:
    betting odds: $< 1/204$

Note that in each of these tests the value of $\frac{\Delta\Gamma}{\Gamma}$ chosen is taken with $\Gamma_s = \Gamma_d$, as is expected in the Standard Model.

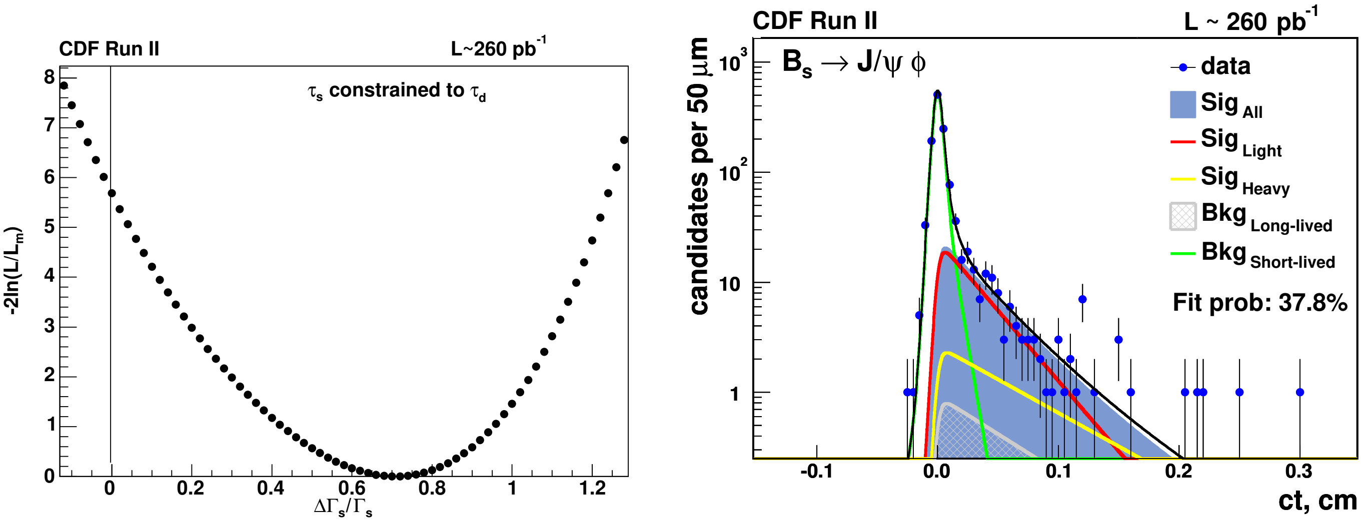

FIG. 9: Scan of the Likelihood function for $\Delta\Gamma_s/\Gamma_s$ for the constrained fit (left) and the projection of the results of the unbinned Likelihood constrained fit onto the data for $B_s \rightarrow J/\psi\phi$ (right).

A. Requiring Equality of the Transversity Amplitudes

The observed B_d and B_s transversity amplitudes (A_0, etc.) are not equal, as might be expected from exact SU(3) flavor symmetry [3]. To see what effect demanding exact SU(3) flavor symmetry would have, additional fits for $\frac{\Delta\Gamma}{\Gamma}$ in the B_s data were performed:

- By fixing the transversity amplitudes in the B_s fit to be the values found in the B_d data — result $\frac{\Delta\Gamma}{\Gamma} = 0.41 \pm 0.20$.
- By fixing the transversity amplitudes in the B_s fit to be the values found in the B_d data AND constraining $\Gamma_s = \Gamma_d$ to within 1% — result $\frac{\Delta\Gamma}{\Gamma} = 0.38 \pm 0.17$.

Evidently, even when requiring exact SU(3) flavor symmetry and the Standard Model assumption that $\Gamma_s = \Gamma_d$ to within 1%, evidence for a lifetime difference remains.

B. $\frac{\Delta\Gamma}{\Gamma}$ Fit Constrained by B_s Semileptonic Decay Lifetime

Averaging of the PDG 2004 results for the observed lifetime in B_s semileptonic decays yields $\tau_{sl} = 430.8 \pm 19.8\mu$m. This is based on four measurements:

- ALEPH: $\tau_{sl} = 1.54\ ^{+0.14}_{-0.13} \pm 0.04$ ps [13]
- CDF: $\tau_{sl} = 1.36 \pm 0.09\ ^{+0.06}_{-0.05}$ ps [14]
- DELPHI: $\tau_{sl} = 1.42\ ^{+0.14}_{-0.13} \pm 0.03$ ps [15]
- and OPAL: $\tau_{sl} = 1.50\ ^{+0.16}_{-0.15} \pm 0.04$ ps [16]

In what follows it is assumed that these are all good measurements of the weighted average of the lifetimes for B_s semileptonic decays (which initally start from an equal mixture of the CP even and odd states) and in principle and in practice are sensitive to decays from lifetime components with lifetimes in the range of 1 to 2 psec. With this assumption the following relationship should hold [17]:

$$\tau_{sl} = \frac{1}{\Gamma_s} \frac{1+\frac{1}{4}(\frac{\Delta\Gamma}{\Gamma})^2}{1-\frac{1}{4}(\frac{\Delta\Gamma}{\Gamma})^2},$$

This relationship can be used as a constraint between Γ_s and $\Delta\Gamma_s$ with the left hand side set (within the uncertainties) to the world average τ_{sl} given above. By redoing the full time-dependent angular fit with this constraint, we find $\frac{\Delta\Gamma}{\Gamma} = 0.4 \pm 0.19$ and $c\tau_s = 1/\Gamma_s = 401 \pm 29\mu$m. Evidently the observed lifetime in B_s semileptonic decays and evidence for two lifetimes in the B_s system can be simultaneously be met if Γ_s is about 15% larger than Γ_d.

VI. CROSS CHECKS

A. CP Odd Fraction vs. a Proper Decay Length Cut in the B_s Sample

A proper decay length (PDL) cut is expected to enhance the fraction of the longer lived component if there is a significant difference between the two lifetimes. By performing a fit without PDL terms in the Likelihood function one obtains the time-integrated fraction as a function of a $c\tau$ cut, as shown in Table IV. Although the uncertainties are large, the agreement is striking and consistent with a long-lived CP odd component.

Cut(μm)	Fitted (%)	Predicted (%)
> 0	20.1 ± 9.0	–20.1–
> 150	24.2 ± 10.3	24.1
> 300	29.6 ± 12.7	28.6
> 450	38.7 ± 11.6	33.6

TABLE IV: CP odd time-integrated fraction vs. a $c\tau$ cut.

The increase of the CP odd fraction suggests a relative large lifetime difference which is consistent with the result from the time dependent angular fit. The expected time-integrated fraction can be derived using the results from the time dependent fit for $c\tau_L$ and $c\tau_H$ and the assumption that the initial CP odd fraction is 20.1%. The comparison is also listed in Table IV.

A similar test for the time-integrated fraction of the parity odd component in the B_d was also performed. As shown in Table V, the parity odd fraction remains unchanged as the $c\tau$ cut is increased.

Cut(μm)	Fitted (%)
> 0	21.6 ± 4.4
> 150	23.0 ± 3.6
> 300	23.0 ± 4.0
> 450	23.6 ± 4.9

TABLE V: B_d parity odd fraction vs. $c\tau$ cut.

B. 'Fitting for Two Lifetimes' Using the B_d Sample

An interesting cross check is to try fitting for two lifetimes in the B_d sample, where no effect is expected. Since the B_d sample is about four times as large as the B_s sample, in addition to the fit on the entire B_d sample, we split the events into four separate sub-samples and repeat the test on each of them. Table VI lists the fitting results, all of which are compatible with zero. It is important to note that these results DO NOT represent a measurement or limit on the size of a potential lifetime difference in the B_d system; this data is insensitive to such an effect. This test is really a technical sanity check that we obtain zero when we expect to do so.

Fit	$\Delta\Gamma/\Gamma(\%)$	$c\tau_L(\mu m)$
Full sample one $c\tau$	–	461 ± 15
Full sample	14.5 ± 12.1	444 ± 21
1st sub sample	13.7 ± 27.9	422 ± 34
2nd sub sample	25.1 ± 22.3	437 ± 39
3rd sub sample	26.1 ± 23.0	437 ± 50
4th sub sample	-7.6 ± 27.6	475 ± 41

TABLE VI: Results of $\Delta\Gamma/\Gamma$ fit using B_d samples.

VII. SYSTEMATIC UNCERTAINTIES

Systematic uncertainties found to have non-negligible effects are due to the modeling of the background shape, particle mis-assignment in the B_d decays ($K-\pi$ interchange), potential contributions from non-resonant $K\pi$ states for the B_d decays, and contamination of the B_s sample from mis-assigned B_d decays. The sculpting of the angular distributions caused by the trigger effciency, detector acceptance and offline selection criteria have been corrected for and the method is found to have negligble residual systematic uncertainties.

B_d^0	$c\tau(\mu\text{m})$	A_0	$A_{\|\|}$	$A_\perp$	$\delta_{\|\|}$	$\delta_\perp$
Bkg. Model	3.9	0.009	0.006	0.006	0.01	0.01
$K\pi$ Swap	–	0.002	0.002	0.002	0.01	0.00
Non-resonant	–	0.007	0.001	0.004	0.07	0.04
Lifetime	2.4	–	–	–	–	–
Total	4.6	0.012	0.006	0.007	0.07	0.04

TABLE VII: Systematic Uncertainties for B_d^0 Results.

B_s^0	$c\tau(\mu\text{m})$	$\Delta\Gamma/\Gamma$	A_0	$A_{\|\|}$	$A_\perp$	$\delta_{\|\|}$
Bkg. Model	3.7	0.007	0.007	0.013	0.003	0.03
B_d cross-feed	5.0	0.008	–	0.003	0.001	–
Lifetime	2.4	–	–	–	–	–
Total	6.7	0.011	0.007	0.013	0.003	0.03

TABLE VIII: Systematic Uncertainties for B_s^0 Results.

Figures 10 and 11 show a comparison of Monte Carlo vs. data for distributions in various physical quantities of interest.

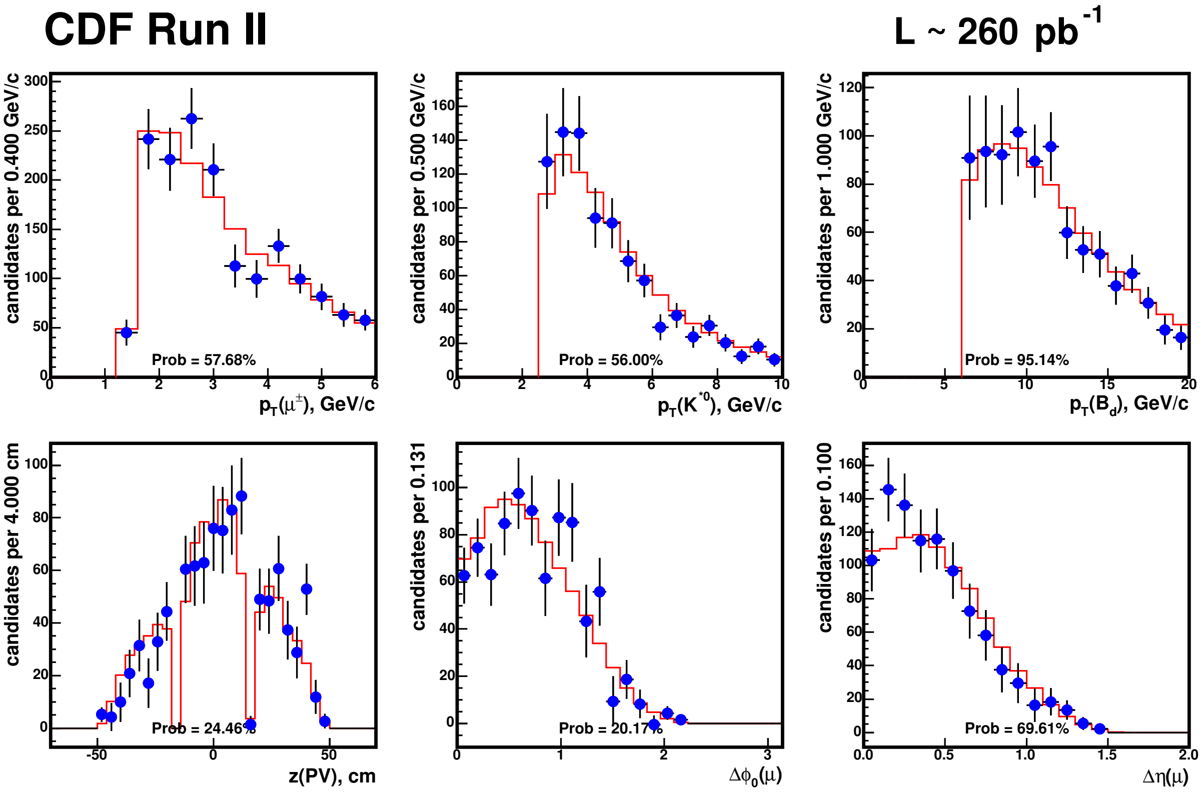

FIG. 10: Comparison of Monte Carlo and data for B_d decays.

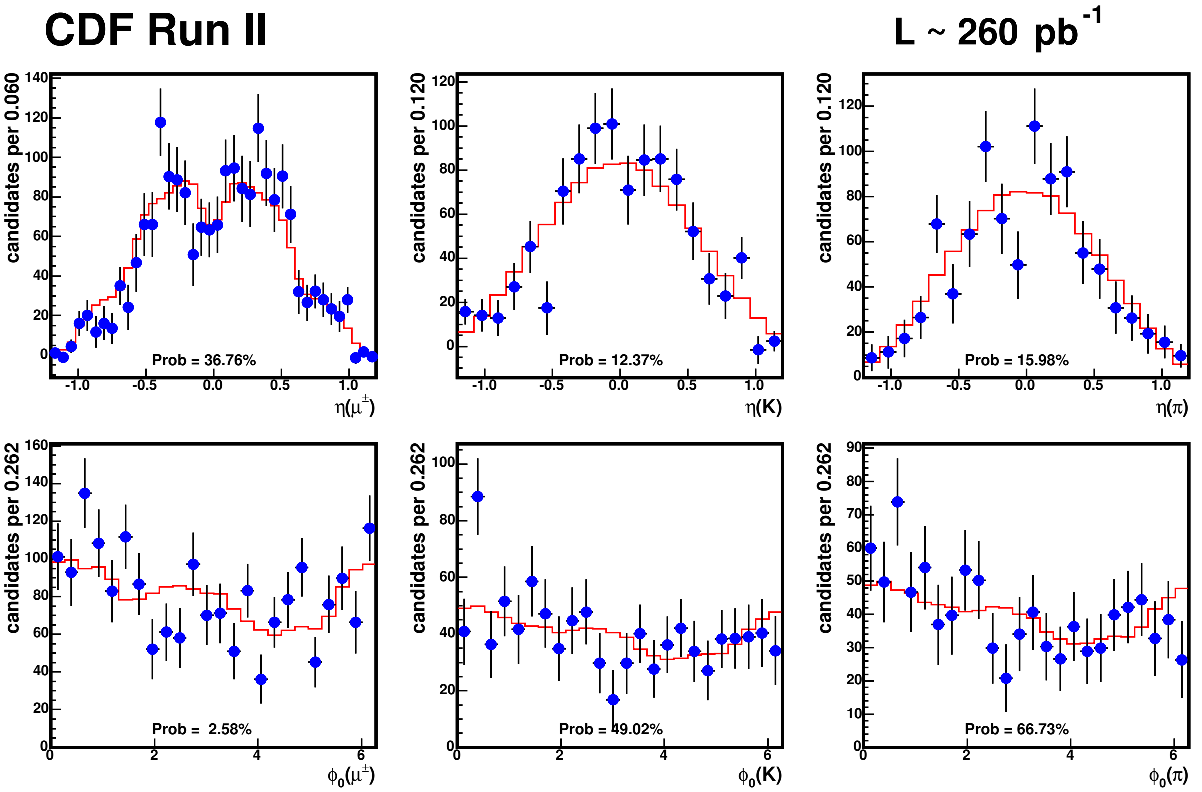

FIG. 11: Comparison of Monte Carlo and data for B_d decays.

VIII. FINAL RESULTS

For B_s, with no constraints we obtain:

$$\begin{aligned}
A_0 &= 0.784 \pm 0.039 \pm 0.007 \\
A_{||} &= (0.510 \pm 0.082 \pm 0.013)e^{(1.94 \pm 0.36 \pm 0.03)i} \\
|A_\perp| &= 0.354 \pm 0.098 \pm 0.003 \\
\tau_L &= 1.05 \,^{+0.16}_{-0.13} \pm 0.02 \text{ ps} \\
\tau_H &= 2.07 \,^{+0.58}_{-0.46} \pm 0.03 \text{ ps} \\
\Delta\Gamma/\Gamma &= 0.65 \,^{+0.25}_{-0.33} \pm 0.01 \\
\Delta\Gamma &= 0.47 \,^{+0.19}_{-0.24} \pm 0.01 \text{ ps}^{-1}
\end{aligned}$$

For B_s with the $\Gamma_s = \Gamma_d$ constraint, we obtain:

$$\begin{aligned}
A_0 &= 0.783 \pm 0.038 \pm 0.007 \\
A_{||} &= (0.539 \pm 0.082 \pm 0.013)e^{(1.91 \pm 0.32 \pm 0.03)i} \\
|A_\perp| &= 0.308 \pm 0.087 \pm 0.003 \\
\tau_L &= 1.13 \,^{+0.13}_{-0.09} \pm 0.02 \text{ ps} \\
\tau_H &= 2.38 \,^{+0.56}_{-0.43} \pm 0.03 \text{ ps} \\
\Delta\Gamma/\Gamma &= 0.71 \,^{+0.24}_{-0.28} \pm 0.01 \\
\Delta\Gamma &= 0.46 \,^{+0.17}_{-0.18} \pm 0.01 \text{ ps}^{-1}
\end{aligned}$$

For B_d, we obtain:

$$\begin{aligned}
A_0 &= 0.750 \pm 0.017 \pm 0.012 \\
A_{||} &= (0.473 \pm 0.034 \pm 0.006)e^{(2.86 \pm 0.22 \pm 0.07)i} \\
A_\perp &= (0.464 \pm 0.035 \pm 0.007)e^{(0.15 \pm 0.15 \pm 0.04)i} \\
\tau_{B^0} &= 1.54 \pm 0.05 \pm 0.02 \text{ ps}
\end{aligned}$$

All of the results obtained are consistent with previously published results. The results for the transversity amplitudes and phases are in very good agreement with previously published results.

The results for the transversity amplitudes and phases obtained for B_d and B_s are shown on the complex plane in Figure 12. Comparison overlays of B_d and B_s results as well as the B_d results from this analysis with those from BaBar [18] and Belle [19], are shown in Figure 13.

A. Implications for Δm_s

Within the Standard Model, it is estimated that $\frac{\Delta\Gamma_s}{\Delta m_s} = (3.7^{+0.8}_{-1.5}) \times 10^{-3}$. To convert the observed value for $\Delta\Gamma_s$ to a value for Δm_s, we use the result from the constrained fit and obtain $\Delta m_s = 125^{+69}_{-55}$, which can be compared to the 95% C.L. lower limit of $\Delta m_s > 14.5\,\text{ps}^{-1}$.

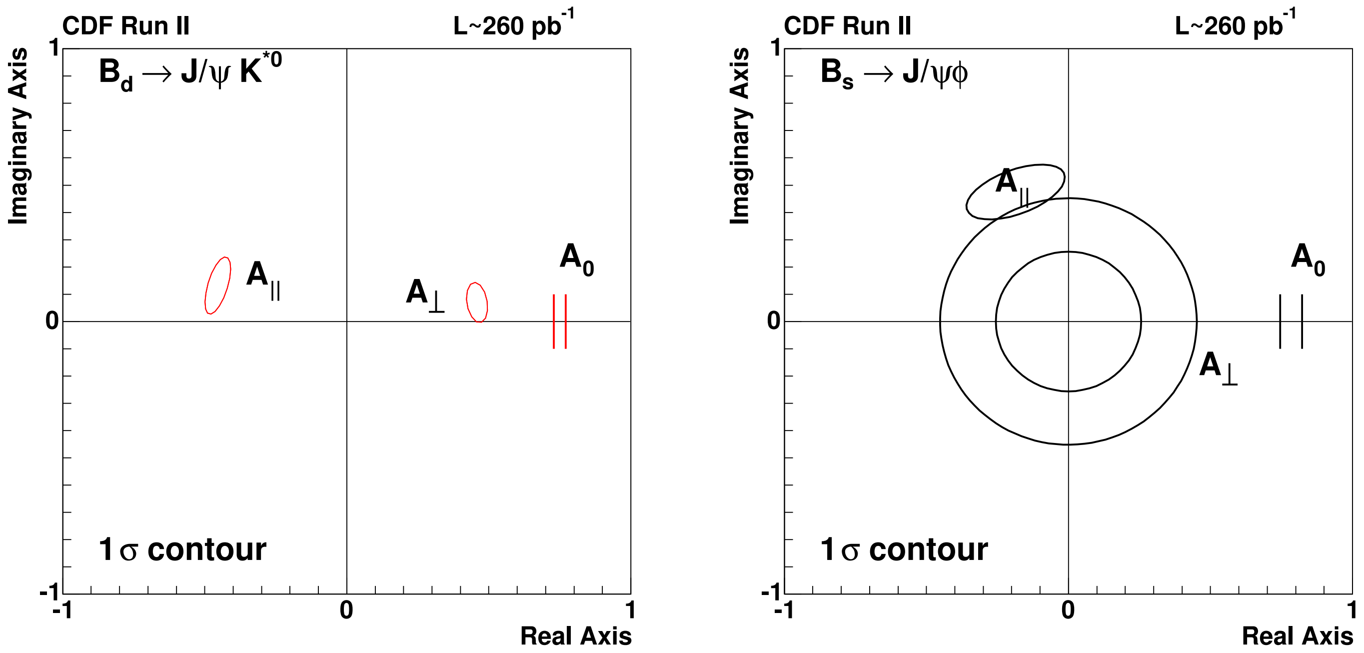

FIG. 12: Argand plot of the transversity amplitudes for B_d and B_s obtained in this analysis.

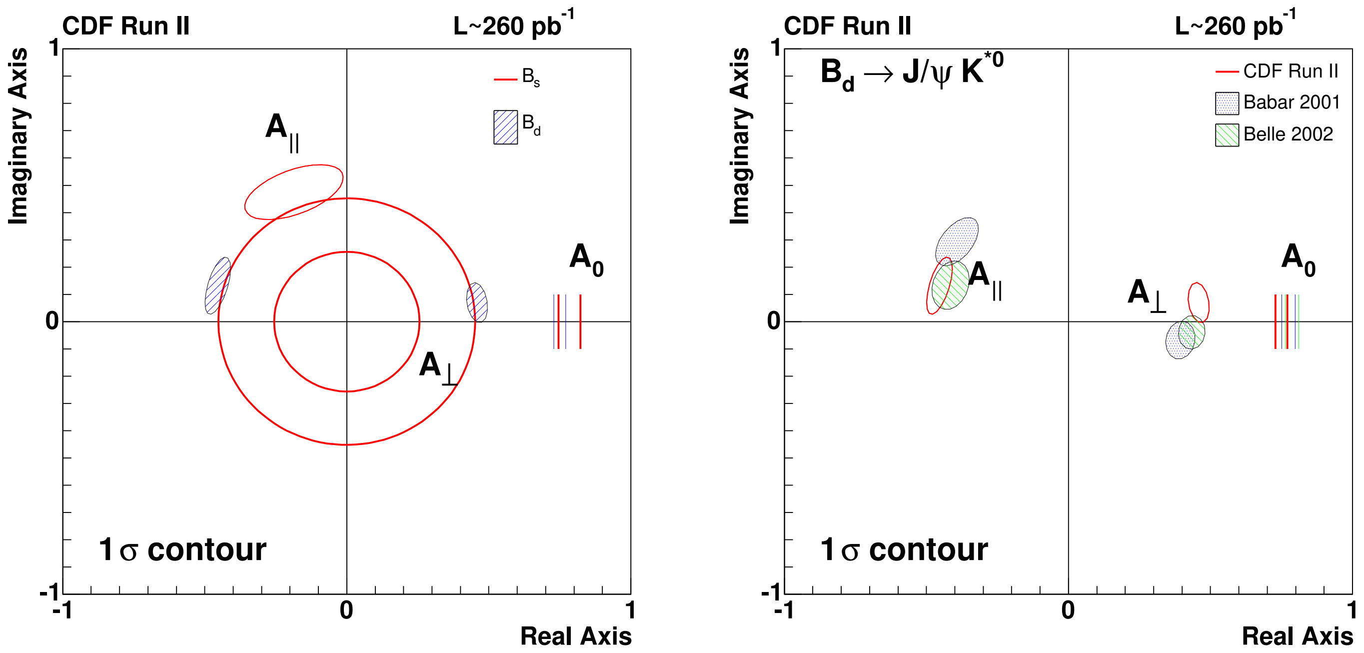

FIG. 13: Argand plots showing an overlay of the transversity amplitudes for B_d and B_s obtained in this analysis (left) and and comparison of the B_d results from this experiment with those obtained by BaBar [18] and Belle [19] (right).

Acknowledgments

We thank the Fermilab staff and the technical staffs of the participating institutions for their vital contributions. This work was supported by the U.S. Department of Energy and National Science Foundation; the Italian Istituto Nazionale di Fisica Nucleare; the Ministry of Education, Culture, Sports, Science and Technology of Japan; the Natural Sciences and Engineering Research Council of Canada; the National Science Council of the Republic of China; the Swiss National Science Foundation; the A.P. Sloan Foundation; the Bundesministerium fuer Bildung und Forschung, Germany; the Korean Science and Engineering Foundation and the Korean Research Foundation; the Particle Physics and Astronomy Research Council and the Royal Society, UK; the Russian Foundation for Basic Research; the Comision Interministerial de Ciencia y Tecnologia, Spain; and in part by the European Community's Human Potential Programme under contract HPRN-CT-20002, Probe for New Physics.

---

[1] I. Bigi *et al.,* in "B Decays", 2nd Edition, edited by S. Stone (World Scientific, Singapore, 1994).
[2] A. Dighe, I. Dunietz and R. Fleischer, Eur. Phys. J. **C6**, 647 (1999).
[3] A.S. Dighe, I. Dunietz, H.J. Lipkin and J.L. Rosner, Phys. Lett. **B369**, 144 (1996).
[4] A. Dighe, T. Hurth, C. Kim, and T. Yoshikawa, Nucl. Phys. **B624**, 377 (2002).
[5] K. Anikeev *et al.*, *B physics at the Tevatron Run II and Beyond*, FERMILAB-Pub-01, 197 (2001).
[6] R. Blair *et al.*,, CDF II Collaboration, FERMILAB-PUB-96/390-E.
[7] T. Affolder *et al.,* FERMILAB-PUB-93/355-E, submitted to Nucl. Instrum. Meth. A.
[8] A. Sill *et al.,* Nucl. Instrum. Meth. A **447**, 1 (2000).
[9] G. Ascoli *et al.,* Nucl. Instrum. Meth. A **268**, 33 (1988).
[10] T. Dorigo *et al.,* Nucl. Instrum. Meth. A **494**, 560 (2001).
[11] E.J. Thomson *et al.,* IEEE Trans. Nucl. Sci. **49**, 1063 (2002).
[12] S. Pappas, *Measurement of the Polarization in* $B \to VV$ *Decays*, doctoral thesis, Yale University (1999) `http://www.lns.cornell.edu/ pappas/thesis/thesis.html`, and T. Affolder *et al.*, CDF Collaboration, Phys. Rev. Lett. **85**, 4668 (2000).
[13] D. Buskulic *et al.*, ALEPH Collaboration, Phys. Lett. **B377** 205 (1996).
[14] K. Abe *et al.*, CDF Collaboration, Phys. Rev.. **D59**, 032004 (1999).
[15] P. Abreu *et al.*, DELPHI Collaboration, Eur. Phys. J. **C16** 555 (2000).
[16] K. Ackerstaff em et al., OPAL Collaboration, Phys. Lett. **B426** 161 (1998).
[17] K. Hartkorn and H.-G. Moser, Eur. Phys. J. **C8**, 381 (1999).
[18] B. Aubert *et al.*, BaBar Collaboration, Phys. Rev. Lett. **87**, 241801 (2001).
[19] K. Abe *et al.*, Belle Collaboration, Phys. Lett. **B538**, 11 (2002).